LOCAL-TIME SURVEY OF PLASMA AT LOW ALTITUDES OVER THE AURORAL ZONES*

by

L. A. Frank and K. L. Ackerson

Department of Physics and Astronomy
THE UNIVERSITY OF IOWA
Iowa City, Iowa

U. of Iowa 71-40

LOCAL-TIME SURVEY OF PLASMA AT LOW ALTITUDES OVER THE AURORAL ZONES*

by

L. A. Frank and K. L. Ackerson

August 1971

Department of Physics and Astronomy
The University of Iowa
Iowa City, Iowa 52240

*Research supported in part by the National Aeronautics and Space Administration under contracts NAS5-10625, NAS1-8141 and NAS1-2973 and grant NGL16-001-002 and by the Office of Naval Research under contract N000-14-68-A-0196-0003.

UNCLASSIFIED

Security Classification

DOCUMENT CONTROL DATA - R&D

(Security classification of title, body of abstract and indexing annotation must be entered when the overall report is classified)

1. ORIGINATING ACTIVITY (Corporate author)
University of Iowa
Department of Physics and Astronomy

2a. REPORT SECURITY CLASSIFICATION
UNCLASSIFIED

2b. GROUP

3. REPORT TITLE

LOCAL-TIME SURVEY OF PLASMA AT LOW ALTITUDES OVER THE AURORAL ZONES.

4. DESCRIPTIVE NOTES (Type of report and inclusive dates)

5. AUTHOR(S) (Last name, first name, initial)

Frank, L. A. and Ackerson K. L.

6. REPORT DATE	7a. TOTAL NO. OF PAGES	7b. NO. OF REFS
August 1971	36	17

8a. CONTRACT OR GRANT NO.
N000-14-68-A-0196-0003

b. PROJECT NO.

c.

d.

9a. ORIGINATOR'S REPORT NUMBER(S)
U. of Iowa 71-40

9b. OTHER REPORT NO(S) (Any other numbers that may be assigned this report)

10. AVAILABILITY/LIMITATION NOTICES

Approved for public release; distribution is unlimited.

11. SUPPLEMENTARY NOTES

12. SPONSORING MILITARY ACTIVITY
Office of Naval Research

13. ABSTRACT

SEE PAGES FOLLOWING

DD FORM 1 JAN 64 1473

UNCLASSIFIED

Security Classification

14. KEY WORDS	LINK A		LINK B		LINK C	
	ROLE	WT	ROLE	WT	ROLE	WT
Aurora						
Magnetosphere						
Plasma Sheet						

INSTRUCTIONS

1. ORIGINATING ACTIVITY: Enter the name and address of the contractor, subcontractor, grantee, Department of Defense activity or other organization *(corporate author)* issuing the report.

2*a*. REPORT SECURITY CLASSIFICATION: Enter the overall security classification of the report. Indicate whether "Restricted Data" is included. Marking is to be in accordance with appropriate security regulations.

2*b*. GROUP: Automatic downgrading is specified in DoD Directive 5200.10 and Armed Forces Industrial Manual. Enter the group number. Also, when applicable, show that optional markings have been used for Group 3 and Group 4 as authorized.

3. REPORT TITLE: Enter the complete report title in all capital letters. Titles in all cases should be unclassified. If a meaningful title cannot be selected without classification, show title classification in all capitals in parenthesis immediately following the title.

4. DESCRIPTIVE NOTES: If appropriate, enter the type of report, e.g., interim, progress, summary, annual, or final. Give the inclusive dates when a specific reporting period is covered.

5. AUTHOR(S): Enter the name(s) of author(s) as shown on or in the report. Enter last name, first name, middle initial. If military, show rank and branch of service. The name of the principal author is an absolute minimum requirement.

6. REPORT DATE: Enter the date of the report as day, month, year; or month, year. If more than one date appears on the report, use date of publication.

7*a*. TOTAL NUMBER OF PAGES: The total page count should follow normal pagination procedures, i.e., enter the number of pages containing information.

7*b*. NUMBER OF REFERENCES: Enter the total number of references cited in the report.

8*a*. CONTRACT OR GRANT NUMBER: If appropriate, enter the applicable number of the contract or grant under which the report was written.

8*b*, 8*c*, & 8*d*. PROJECT NUMBER: Enter the appropriate military department identification, such as project number, subproject number, system numbers, task number, etc.

9*a*. ORIGINATOR'S REPORT NUMBER(S): Enter the official report number by which the document will be identified and controlled by the originating activity. This number must be unique to this report.

9*b*. OTHER REPORT NUMBER(S): If the report has been assigned any other report numbers *(either by the originator or by the sponsor)*, also enter this number(s).

10. AVAILABILITY/LIMITATION NOTICES: Enter any limitations on further dissemination of the report, other than those imposed by security classification, using standard statements such as:

(1) "Qualified requesters may obtain copies of this report from DDC."

(2) "Foreign announcement and dissemination of this report by DDC is not authorized."

(3) "U. S. Government agencies may obtain copies of this report directly from DDC. Other qualified DDC users shall request through _____."

(4) "U. S. military agencies may obtain copies of this report directly from DDC. Other qualified users shall request through _____."

(5) "All distribution of this report is controlled. Qualified DDC users shall request through _____."

If the report has been furnished to the Office of Technical Services, Department of Commerce, for sale to the public, indicate this fact and enter the price, if known.

11. SUPPLEMENTARY NOTES: Use for additional explanatory notes.

12. SPONSORING MILITARY ACTIVITY: Enter the name of the departmental project office or laboratory sponsoring *(paying for)* the research and development. Include address.

13. ABSTRACT: Enter an abstract giving a brief and factual summary of the document indicative of the report, even though it may also appear elsewhere in the body of the technical report. If additional space is required, a continuation sheet shall be attached.

It is highly desirable that the abstract of classified reports be unclassified. Each paragraph of the abstract shall end with an indication of the military security classification of the information in the paragraph, represented as *(TS)*, *(S)*, *(C)*, or *(U)*.

There is no limitation on the length of the abstract. However, the suggested length is from 150 to 225 words.

14. KEY WORDS: Key words are technically meaningful terms or short phrases that characterize a report and may be used as index entries for cataloging the report. Key words must be selected so that no security classification is required. Identifiers, such as equipment model designation, trade name, military project code name, geographic location, may be used as key words but will be followed by an indication of technical context. The assignment of links, roles, and weights is optional.

Abstract

A local-time survey of the low-energy proton and electron intensities precipitated into the earth's atmosphere over the auroral zones during periods of magnetic quiescence has been constructed by selecting a typical, individual satellite crossing of this region in each of eight local-time sectors from a large library of similar observations with the polar-orbiting satellite Injun 5. The trapping boundary for more energetic electron intensities, $E > 45$ keV, was found to be a 'natural coordinate' for delineating the boundary between the two major types of lower energy, $50 \leq E \leq 15{,}000$ eV, electron precipitation commonly observed over the auroral zones at low altitudes. Poleward of this trapping boundary inverted 'V' electron precipitation bands are observed in all local-time sectors. These inverted 'V' electron bands are typically more energetic and of greater latitudinal width in the evening and midnight sectors relative to their counterparts in the noon and morning sectors. Equatorward of the trapping boundary the electron energy influx is dominated by plasma sheet electron intensities in the midnight and early morning sectors. Precipitation of ring current proton intensities is most often observed in the late evening sector and equatorward of the major regions

of electron influx. In general the main contributors to the electron energy influx into the earth's atmosphere over the auroral zones are the electron inverted 'V' precipitation poleward of the trapping boundary in late evening, the plasma sheet electron intensities equatorward of this boundary in early morning and both types of these precipitation events near local midnight. These observations of low-altitude charged particle intensities are interpreted favorably in terms of a current magnetospheric model and compared with similar measurements in the distant magnetosphere.

I. Introduction

During the past several years or so a wealth of new observations of low-energy particle intensities and of associated phenomena over the earth's auroral zones as gained with low-altitude polar-orbiting satellites has become available. Correspondingly the classification of the various plasma regimes, e.g., 'soft' and 'hard' zones and 'burst' regions, has become increasingly more complex. Often these zones are identified by finding ratios of responses of a particular detector at, say, two different energy channels or by the overall variability of the instrument response with respect to time or latitude. A collection of instruments with differing and/or limited capabilities will in turn provide a plethora of plasma regions often confusing to all but observers directly involved in this work.

The large temporal and spatial fluctuations of low-energy charged particle intensities over the auroral zones are further major obstacles in interpretation of the observations. Efforts in statistical studies of the spatial distributions of these plasmas as functions of latitude and magnetic activity, for example, have yielded a substantial inventory of important results. Hoffman [1971b] has recently given a review of many of the most current of these studies.

However, many of the details and interrelationships of the plasma regimes are unresolved in these statistical studies. For a detailed description of auroral plasma phenomena we need also to find the precise spatial interrelationships of the 'trapping boundary' for more energetic electrons ($E \geq 40$ keV), the plasma sheet, the ring current and the magnetosheath as observed at auroral altitudes. Without simultaneous measurements of electron and proton intensities over a generous energy range it is almost, if not, impossible to provide this information.

Our present interest is directed toward a local-time survey of proton and electron intensities over the Northern auroral zones and polar cap which has been obtained by selecting an individual, typical observation in each local-time sector during periods of relative magnetic quiescence. As we shall see these simultaneous measurements of proton and electron intensities, together with the local determination of the 'trapping boundary' for more energetic electrons, provide a unique insight into the distributions and interrelationships of the plasma regimes over the auroral zones. Although individual precipitation patterns are often complex, the overall spatial distributions of low-energy charged particle intensities over the auroral zones are relatively easily associated with plasma domains of the distant magnetosphere and its environs.

II. Observations

An array of electrostatic analyzers capable of measuring simultaneously the directional, differential energy spectrums of proton and electron intensities precipitated into and trapped above the auroral zones was launched with the satellite Injun 5 into a low-altitude, polar orbit on 8 August 1968. The spacecraft was magnetically aligned with the local geomagnetic field by means of two parallel permanent bar magnets. Over the Northern hemisphere the spacecraft was often commanded into an operating mode which provided 117-sample differential energy spectrums of proton and electron intensities at local pitch angles $\alpha = 0°$ and $90°$ in a 970-millisecond sampling interval once each two seconds. The energy ranges of these electrostatic analyzers, or LEPEDEA's, were $40 \leq E \leq 12{,}000$ eV and $50 \leq E \leq 15{,}000$ eV for proton and electron intensities, respectively. In addition a complement of collimated, thin-windowed Geiger-Mueller tubes was employed to determine the location of the 'trapping boundary' for more energetic electron intensities with $E > 45$ keV. Further description of the satellite and its instrumentation has been given by Frank and Ackerson [1971].

We have chosen a series of eight passes over the auroral zones for our present summary of the local-time distributions of proton and electron intensities observed at

low altitudes. These particular series of measurements were selected from a large library of such observations on the basis of (1) relative magnetic quiescence for the observing period as indicated by K_p and D_{ST} (H), (2) continuous telemetry coverage spanning the outer radiation zone through the auroral precipitation zone and into the polar cap, and (3) features of the plasma distributions which were commonly observed during other passes in a given local-time sector. The results of this survey are displayed in Plates 1a and 1b for precipitating electron and proton intensities, respectively.

Before discussing the contents of Plates 1a and 1b we remind the reader here of the nature of the E-t spectrograms employed to display the massive body of individual intensity measurements gained during a ten-minute observing period over the auroral zones. The ordinate scale of each spectrogram is electron (or proton) energy in units of eV and the abscissa is Universal Time [Frank and Ackerson, 1971]. The detector response is color-coded from blue to red (low to high responses) at each point in the E-t plane. A color calibration strip for the $\log_{10}$ of the detector response in counts $(\text{second})^{-1}$ is provided at the right-hand side of each spectrogram. Magnetic invariant latitudes Λ of the satellite position are to be found along the abscissas of the spectrograms. These spectrograms each span a period of ten minutes

and comprise approximately 30,000 individual intensity measurements. Typical differential energy spectrums for similar spectrograms have been previously published [Frank and Ackerson, 1971; Ackerson and Frank, 1971]. However, we are specially interested here in the overall character of the proton and electron distributions over the auroral zones as gained via these high-resolution spectrograms.

The spectrograms of Plates 1a and 1b are positioned approximately according to the magnetic local time of the observation. For example, Revolutions 3958 and 3667 encountered the auroral zone near local noon and midnight, respectively. The position of the satellite for each E-t spectrogram in the invariant latitude-magnetic local time coordinate system is given in the center panel of each color plate. The interval between each solid circle along a given trajectory line represents an elapsed time of one minute in the corresponding spectrogram. The auroral oval as determined by Feldstein [1963] from ground-based observations is indicated by the shaded area in the Λ-MLT grid and is included for comparison with the spatial coverage provided by the E-t spectrograms.

The 'trapping boundary' for more energetic electrons $E > 45$ keV as gained via a thin-windowed Geiger-Mueller tube with collimated field-of-view directed perpendicular to the

local magnetic field is indicated by the arrows at the bottom of each spectrogram and in the Λ-MLT coordinates of the center panel. The width of the shaft of each arrow represents the uncertainty in the determination of this boundary. A summary of these measurements is given in Figure 1. This 'trapping boundary' is defined as coincident with the high latitude termination of measurable electron intensities. For example, this boundary is located at $\Lambda = 75°$ for Revolution 3541. The counting rates above threshold at high latitudes during Revolutions 1486 and 1487 are attributable to the entry of energetic solar protons into the earth's polar cap. The intensity maximum centered at $\Lambda = 76°$ during Revolution 1486 is the G. M. tube response to solar X-rays as the direction to the sun passes through its field-of-view. Two electron precipitation events poleward of the trapping boundary were sufficiently energetic such that the high-energy tail of the electron spectrums was observable in the G. M. tube responses. These two events are evident at $\Lambda \simeq 72$ to $73.5°$ for Revolution 3667 and $\Lambda \simeq 71$ to $73°$ for Revolution 1487. It is useful to compare these measurements with the lower energy electron precipitation events shown in Plate 1a. The well-known diurnal variation in the location of the trapping boundary is evident even for the limited selection of examples shown in Figure 1. This boundary

is positioned at significantly higher latitudes during local day (Revolutions 5410, 1486 and 3958) relative to those at local night (Revolutions 1487, 3667 and 5799).

Frank and Gurnett [1971] have recently shown that the position of the trapping boundary in the local dawn and evening sectors is coincident within observational errors with the reversal of convection electric fields from sunward convective flow (equatorward of the trapping boundary) to anti-sunward flow (poleward of this boundary). On the basis of recent measurements of plasmas and wave phenomena in the distant and near-earth polar magnetosphere, we have also interpreted the position of the trapping boundary as delineating the location of the high-latitude termination of closed field lines, i.e., all field lines above the trapping boundary are directly connected to the interplanetary magnetic field [Frank, 1971b, c; Frank and Gurnett, 1971; Gurnett and Frank, 1971a, b; Ackerson and Frank, 1971]. The usefulness and effectiveness of this trapping boundary as an *in situ* coordinate for the above studies have led us in recent past investigations and the present study to employ it as a 'natural coordinate'.

Returning to the observations of precipitated low-energy proton and electron intensities as displayed in Plates 1a and 1b we find a discussion most easily implemented

by first noting the general character of the plasma distributions poleward of the trapping boundary as a function of local time and concluding with a similar description of observations equatorward of this boundary. Pertinent dates, altitudes and magnetic indices K_p and D_{ST} (H) for each E-t spectrogram are given in Table I.

Poleward of the trapping boundary. As an aid to the reader in interpretation of the series of E-t spectrograms of Plates 1a and 1b a single set of proton and electron spectrograms is first discussed in detail. Inspection of Plate 1b reveals that a band of low-energy proton intensities is observed poleward of the trapping boundary on the local-day sector of the auroral precipitation pattern. For example, a band of these proton intensities is observed at 2331:00 to 2332:10 U.T. during Revolution 1486. The trapping boundary was intersected at 2330:50 U.T. during this northbound pass. These proton intensities have been previously interpreted as the low-altitude signature of the polar cusp and hence of the direct entry of magnetosheath plasma into the polar magnetosphere [cf. Frank and Ackerson, 1971; Frank, 1971b, c; Heikkila and Winningham, 1970]. The proton intensities are considerably less than those observed in the direction of flow within the magnetosheath. Gurnett and Frank [1971a] have also shown previously that a strong

Table I.

Dates, Magnetic Indices and Altitudes for

E-t Spectrograms, Plates 1a and 1b

Revolution Number	Date	K_p	D_{ST} (H),* gammas	Altitude at Midpoint of Spectrogram, kilometers
1486	8 Dec, 1968	3	-32	2320
1487	9 Dec, 1968	1^+	-26	2490
1561	15 Dec, 1968	2	-7	2510
3541	26 May, 1969	1^+	+5	1820
3667	6 June, 1969	0	+18	2470
3958	30 June, 1969	1	+17	2370
5410	27 Oct, 1969	2	+9	2075
5799	28 Nov, 1969	2, 1^+	-9, -11	2540

*After Sugiura and Poros [1971].

eastward convection of plasma, 1.5 to 3.0 km $(\text{second})^{-1}$, as measured simultaneously with a DC electric field instrument, occurs coincident with this band of proton intensities. Measurable intensities of low energy electrons are observed within this band of proton intensities and are bounded at the equatorward side by the relatively intense, thin 'spike' of intensities encountered at 2331:00 U.T. (see Plate 1a). On the other hand, a relatively broader electron precipitation zone with higher average electron energies is located equatorward of the trapping boundary at 2327:20 to 2330:50 U.T. No measurable intensities of precipitated protons are observed equatorward of the trapping boundary for this particular series of observations. The polar cap proper was encountered poleward of the polar cusp at 2332:10 U.T. during Revolution 1486 and is characterized usually by a relative absence of charged particle intensities within the energy range of the E-t spectrograms. Examination of other spectrograms in Plates 1a and 1b reveals a similar void as the trajectories penetrate into the polar cap.

An inventory of the overall character of the E-t spectrograms as a function of local time of the observation reveals the following major results for the precipitation zones poleward of the trapping boundary.

(1) The narrow intense bands of electron intensities

observed above the trapping boundary (e.g., at 0416:40 U.T. of Revolution 3958 and at 2331:00 U.T. of Revolution 1486) increase in width and peak average energies as the local time of the observation passes through local evening to midnight. The signature of the precipitation band at 0149:30 to 0150:10 U.T. of Revolution 1487 is that of an 'inverted V' with the average energy of electrons increasing to a maximum energy and subsequently decreasing as the satellite traverses this electron precipitation event. Although often these precipitation events do not have the remarkable symmetry or rise sufficiently in average energy to reproduce this clear signature as for this particular event, the maximum directional intensities of typically 10^9 to 10^{10} electrons $(cm^2\text{-sec-sr})^{-1}$, their position above the trapping boundary and the well-defined 'spike-like' signature led us to classify the entire family of these precipitation bands as inverted 'V' events. Correspondingly it is implicitly assumed that these precipitation bands have a common origin and that the acceleration mechanism responsible for these precipitation events increases in effectiveness as local time increases through local

evening to the midnight sector. It should be remarked here that although the peak energy fluxes within the inverted 'V' precipitation bands differ by almost three orders of magnitude, the directional intensities of electrons differ by significantly lesser factors, ≤ 10. For example, the peak directional intensities for the event centered at 0623:10 U.T. of Revolution 3667 are within a factor of 2 equal to the peak intensities at 2331:00 U.T. of Revolution 1486.

(2) In the dawn sector these inverted 'V' precipitation bands are often more narrow with lower maximum average electron energies relative to their counterparts at local evening. Examples of these electron precipitation events in early local morning are located at 1157:00, 1158:00 and 1201:50 U.T. for Revolution 5799. These precipitation bands do not largely differ in character from those observed in the noon sector. We have examined our library of these inverted 'V' events in the morning sector during periods of greater magnetic disturbance than those covered in these series of observations and found that these bands do indeed develop into events similar to those reported here in the evening sector (cf. Revolution 1487 of Plate 1a). Hence we would conclude that the acceleration mechanism

associated with these inverted 'V' events is often significantly more effective in the evening and midnight sectors relative to the morning sector (compare the event at 0343:15 to 0344:20 U.T. of Revolution 1561 with that of Revolution 5799 at 1201:50 U.T.).

(3) Multiple inverted 'V' precipitation bands of electron intensities are most frequently observed in the late evening, early morning and midnight sectors of the auroral precipitation pattern. For example, there are three inverted 'V' bands in the spectrogram for Revolution 1487, centered at 0148:10, 0148:40 and 0149:50 U.T.

(4) Often, but not always, an inverted 'V' electron precipitation band is positioned at or slightly poleward of the trapping boundary for more energetic electron intensities (eg., 2331:00 U.T. of Revolution 1486, 0624:30 U.T. of Revolution 3667 and 2126:00 U.T. of Revolution 3541).

(5) Measurable, but relatively weak, magnetosheath proton intensities are observed above the trapping boundary in the local day sectors almost without exception. (Refer to Revolution 3541 at 2125:20 to 2126:30 U.T. and Revolution 3958 at 0415:40 to 0417:00 U.T., Plate 1b.)

(6) Less frequently, magnetosheath protons are observed within the early morning and midnight sectors. Examples of these events are evident at 0623:15 to 0623:40 U.T. of Revolution 3667 and the more diffuse band at ~ 1201:00 to 1203:00 U.T. of Revolution 5799. Proton intensities precipitating into the evening sector are also present in the corresponding spectrogram for Revolution 1561.

(7) Low-energy proton precipitation bands are also often located at the trapping boundary in the midnight and early morning sectors, e.g., at 0624:20 U.T. of Revolution 3667 and 1203:20 U.T. of Revolution 5799. Although it is possible that these intensities are of ionospheric origin their spatial location and isotropic angular distributions (i.e., intensities within factors of 2 or 3 for $\alpha = 0°$ and 90°) lead us to conclude that these proton bands are also to be identified as having their origins within the downstream magnetosheath, perhaps at a stagnation point in convective flow located in the vicinity of the trapping boundary.

(8) When well-defined bands of relatively high proton intensities, such as those centered at 0345:15 U.T. of Revolution 1561 and 0623:20 U.T. of Revolution

3667, are discernible in the proton spectrograms, their position is not coincident with the location of maximum average electron energy, and peak energy fluxes, in an inverted 'V' event but is observed to be directly adjacent to or seemingly detached from the position of maximum electron energy fluxes. Relative to the highly variable character of the electron spectrums, there appears to be no signature of an equally effective acceleration mechanism for protons.

Equatorward of the trapping boundary. The largest intensities of precipitated low-energy protons and electrons equatorward of the trapping boundary are generally observed in the late evening, early morning and midnight sectors of the auroral precipitation patterns. These charged particle intensities delineate the low-altitude projection of the distant plasma sheet and its earthward extension, the proton ring current [cf. Ackerson and Frank, 1971; Frank, 1971a]. The major features of the precipitation patterns equatorward of the trapping boundary as displayed in Plates 1a and 1b are summarized as follows.

(1) Examination of the electron precipitation zones for the series of measurements for local midnight through local morning to noon reveal that these zones progressively become weaker in intensities with increases in average electron energies. Several partial

segments of this electron precipitation zone are characterized by increasing average electron energies with decreasing latitude (e.g., the intervals 2329:00 to 2330:50 U.T. of Revolution 1486 and 1240:10 to 1241:00 U.T. of Revolution 5410). We interpret these observations of electron intensities as the signature of injection of plasma sheet electrons into the midnight sector of the magnetosphere and their subsequent eastward drift accompanied by energization and dissipation into the atmosphere. Hoffman [1971a] has recently arrived at a similar conclusion with observations of electron intensities within several energy bandpasses at $E \geq 700$ eV. It is of interest to compare the peak electron energy fluxes into the atmosphere for the plasma sheet zone equatorward of the trapping boundary and the most energetic of the inverted 'V' events displayed in the spectrogram for Revolution 3667 in Plate 1a. These maximum energy fluxes were 6 ergs $(cm^2\text{-sec-sr})^{-1}$ at 0626:30 U.T. (plasma sheet) and 20 ergs $(cm^2\text{-sec-sr})^{-1}$ at 0623:08 U.T. (inverted 'V' event). The reader is cautioned here that the contents of individual spectrograms should not be taken as 'average values' but as a guide to the relative magnitudes and spatial relationships. These particular energy fluxes were probably higher

than the average intensities observed in this local time sector. In the evening sector of the precipitation zone equatorward of the trapping boundary the measurable electron intensities are restricted to a relatively narrow zone adjacent to the trapping boundary (e.g., at 0150:10 to 0151:00 U.T. of Revolution 1487).

(2) Precipitation of 'ring current' proton intensities is most often observed in the late evening sector. An example of this precipitation is given in the E-t spectrogram for Revolution 1487 at ~ 0150:30 to 0151:10 U.T. in Plate 1b. A comparison of Plates 1a and 1b shows that the ring current is observed to extend to slightly lower latitudes than the electron intensities of the plasma sheet in this local time sector in agreement with surveys at the magnetic equator [cf. Frank 1971a, Ackerson and Frank, 1971]. Utilizing a similar argument as that applied to the electron intensities in the morning sector, we interpret these 'ring current' proton intensities in terms of the westward drift and subsequent energization of plasma sheet proton intensities from the midnight sector. An example of proton intensities in the midnight sector is given in the spectrogram for

Revolution 3667 at 0625:00 to 0626:10 U.T. Precipitation of proton intensities equatorward of the trapping boundary in the afternoon sectors is discernible at 2123:50 to 2124:40 U.T. of Revolution 3541 and at 0412:00 to 0413:00 U.T. of Revolution 3958. (The band at 2118:00 to 2120:00 U.T. of Revolution 3541 is attributable to the detector's background response to large intensities of outer zone energetic electrons.) The two proton bands, one equatorward and the other poleward of the trapping boundary, often observed in the local-day sector of the precipitation pattern are almost certainly to be identified with the two proton zones previously reported by Sharp and Johnson [1968]. The E-t spectrograms for Revolutions 3541 and 3958 represent two useful examples.

(3) Low-energy proton precipitation is found also in the morning sector, e.g., at 1236:50 to 1238:40 U.T. of Revolution 5410. This proton zone is coincident with a diffuse band of low energy electrons displayed in the corresponding spectrogram of Plate 1a. The overall character of this precipitation region suggests that these charged particles may not have been convected in from the plasma sheet in the midnight sector but instead have gained entry along the

flanks of the magnetosphere. With regards to local morning-evening asymmetries it is of interest to note that proton precipitation is often found equatorward of the major electron precipitation events in the evening sector (Revolutions 1487, 1561 and 3541) and generally, but not always, within the overall electron precipitation at local morning and midnight (Revolutions 3667, 5799 and 5410). This feature, along with the pronounced local-time asymmetry of the two major electron precipitation zones, will tend to confuse any statistical study of proton and electron aurora from ground-based and aircraft measurements which is directed toward deducing the corresponding source region in the distant magnetosphere [cf. Eather and Mende, 1971].

III. Discussion

We have presented a survey of the spatial distributions of low-energy proton and electron intensities precipitating into the earth's upper atmosphere over the Northern hemisphere as constructed by selecting a typical, individual measurement in each local-time sector for periods of relative magnetic quiescence from a considerably larger library of such observations. This series of individual satellite passes over the auroral zones has been organized as a function of local time and displayed in Plates 1a and 1b. A detailed discussion of results has been given in the previous section.

Briefly, and partially with the expense of oversimplification, the overall character of the charged particle distributions over the auroral zone can be described in terms of two major precipitation zones, one located poleward and the other located equatorward of the trapping boundary for more energetic electron ($E > 45$ keV) intensities. Poleward of the trapping boundary the electron precipitation pattern is dominated by inverted 'V' precipitation bands which are characterized by increasing average electron energies to a maximum energy with a subsequent decrease in average energy as the satellite passes through these precipitation events.

These inverted 'V' bands are characterized by a narrow width, ~ 10 to 50 km, and lower peak average electron energies, ~ several hundred eV, in the noon sector relative to their counterparts in the late evening and midnight sectors. These inverted 'V' events display an increasing peak average energy, latitudinal width and multiplicity as local time increases from noon through evening to midnight. Inverted 'V' electron precipitation bands are also observed poleward of the trapping boundary in the morning sector. However, a dawn-dusk asymmetry is evident with the inverted 'V' bands at local morning typically characterized with lower peak average electron energies and lesser latitudinal width relative to those located at local evening during periods of relative magnetic quiescence. Often an inverted 'V' precipitation band is located at or just poleward of the trapping boundary. Low-energy protons of magnetosheath origin are observed poleward of the trapping boundary in the sunlit hemisphere of the proton precipitation patterns. These proton intensities are also often observed in the local night sectors and are frequently accompanied by substantially more intense bands of intensities with latitudinal widths ~ 50 to 150 km. These relatively intense proton bands are not coincident with the inverted 'V' electron precipitation events.

Equatorward of the trapping boundary, the most intense

electron precipitation occurs in the midnight and early morning sectors. These electron intensities are identified with those of the plasma sheet by means of their spatial location, overall intensities and average energies, and relatively broad energy spectrums. This electron precipitation zone becomes less intense with increasing average electron energy as the local time of the observation increases through morning to local noon. The origin of this precipitation zone almost certainly is identified as injection of plasma sheet electrons in the local midnight sector and as subsequent eastward drift accompanied by energization and by dissipation into the atmosphere. On the other hand, the precipitated electron intensities in the evening sector are confined to a relatively narrow, $\sim 1°$ to $2°$, band located adjacent to the trapping boundary. Ring current proton intensities are most often observed to precipitate in the evening sector and can be observationally identified with the earthward extension of the plasma sheet. A coarse interpretive diagram of these major features of spatial distributions of low-energy proton and electron intensities and their relationships to the trapping boundary, magnetic field topology and convection zones is given in Figure 2. The inverted 'V' precipitation events occur above the trapping boundary in the zone of strong anti-sunward convection and the precipitation of plasma

sheet charged particle intensities is located equatorward of this boundary in the region of sunward convection. The reader is reminded here that the convection diagram represents the 'average' spatial distributions of convection electric fields measured with the Injun 5 DC electric field instrument. The polar cap proper is a relatively small region usually characterized with an absence of low-energy charged particle intensities and with weak convective flow. However, examples of strong convective flow over an entire trajectory over the polar cap have been also reported [Cauffman and Gurnett, 1971a, b; Maynard, 1971]. Further observational evidences which lend support to the various interpretive features of Figure 2 have been previously presented [Frank 1971a, b, c; Frank and Ackerson, 1971; Gurnett and Frank 1971a, b; Ackerson and Frank, 1971; Frank and Gurnett, 1971; Cauffman and Gurnett, 1971a, b].

We have used the term 'soft electrons' for the electron spectrums observed poleward of the trapping boundary. However, it is quite apparent from the observations presented here that the peak average electron energies in the center of inverted 'V' events, more specifically those located in the late local evening and midnight sectors, can exceed average electron energies for the plasma sheet electron intensities positioned below the trapping boundary. Plasma

sheet electron spectrums are typically broader with integral, directional intensities less by factors of ≥ 10 relative those of the inverted 'V' precipitation bands. Ackerson and Frank [1971] have suggested recently that the plasma sheet proton and electron intensities can be interpreted as the accumulated 'debris' from inverted 'V' electron events in the vicinity of the trapping boundary. This 'debris' becomes trapped on recently reconnected field lines along the magnetotail and is subsequently convected earthward.

The trapping boundary for electron ($E > 45$ keV) intensities has been employed herein as a 'natural coordinate' due to its coincidental position with respect to that of the reversal in convection electric fields and of the demarcation line between the two major types of low-energy electron precipitation as identified with the present series of measurements. This low-altitude trapping boundary is not observationally identical to the equatorial trapping boundary recently utilized by Frank [1971] in his survey of the earthward edge of the plasma sheet near local midnight with the satellite OGO-3. The equatorial boundary was identified with the position of the major rapid decrease of electron intensities with increasing radial distance. The directional intensities of electron ($E > 45$ keV) beyond this boundary and in the plasma sheet typically exceed the intensity thresholds of the

G. M. tubes flown on both OGO 3 and Injun 5. This equatorial trapping boundary was assumed to be coincident with, or in the near vicinity of, the position at which the local magnetic field begins to largely differ from a dipolar field. Hence the low-altitude trapping boundary, defined here as coincident with the high-latitude termination of measurable intensities, is located poleward of the positions of field lines threading the plasma sheet.

With regard to ground-based observations of aurora it is of interest to note briefly the dominant sources of the precipitated electron intensities in the local-night sector. During periods of relative magnetic quiescence the principal energy influx is provided by inverted 'V' electron events poleward of the trapping boundary in the late evening sector and by plasma sheet electrons equatorward of this boundary in the early morning sector. Near local midnight both types of precipitation are often competitive with the inverted 'V' events located poleward of the latitudinally wider plasma sheet precipitation zone.

Acknowledgments

This research was supported in part by the National Aeronautics and Space Administration under contracts NAS5-10625, NAS1-8141, NAS1-2973 and grant NGL16-001-002 and by the Office of Naval Research under contract N000-14-68-A-0196-0003.

References

Ackerson, K. L. and L. A. Frank, Correlated satellite measurements of low-energy electron precipitation and ground-based observations of a visible auroral arc; J. Geophys. Res. (submitted for publication), 1971.

Cauffman, D. P. and D. A. Gurnett, Double probe measurements of DC electric fields with the Injun 5 satellite; J. Geophys. Res. (accepted for publication), 1971a.

Cauffman, D. P. and D. A. Gurnett, Satellite measurements of magnetospheric convection; Space Sci. Rev. (submitted for publication), 1971b.

Eather, R. H. and S. B. Mende, High latitude particle precipitation, and source regions in the magnetosphere; presented at the Advanced Study Institute on Magnetosphere-Ionosphere Interactions, Dalseter, Norway, April, 1971.

Feldstein, Y. I., Some problems concerning the morphology of auroras and magnetic disturbances at high latitudes; Geomagnetizm i Aeronomiya, 3, 183-192, 1963.

Frank, L. A., Relationship of the plasma sheet, ring current, trapping boundary, and plasmapause near the magnetic equator and local midnight; J. Geophys. Res., 76, 2265-2275, 1971a.

Frank, L. A., Comments on a proposed magnetospheric model; J. Geophys. Res., 76, 2512-2515, 1971b.

Frank, L. A., Plasma in the earth's polar magnetosphere; J. Geophys. Res., 76, 5202-5219, 1971c.

Frank, L. A. and K. L. Ackerson, Observations of charged particle precipitation into the auroral zone; J. Geophys. Res., 76, 3612-3643, 1971.

Frank, L. A. and D. A. Gurnett, On the distributions of plasmas and electric fields over the auroral zones and polar caps; J. Geophys. Res. (accepted for publication), 1971.

Gurnett, D. A. and L. A. Frank, VLF hiss and related plasma observations in the polar magnetosphere; J. Geophys. Res. (submitted for publication) 1971a.

Gurnett, D. A. and L. A. Frank, ELF noise bands associated with auroral arcs; J. Geophys. Res. (submitted for publication), 1971b.

Heikkila, W. J. and J. D. Winningham, Penetration of magnetosheath plasma to low altitudes through the dayside magnetospheric cusps; J. Geophys. Res., 76, 883-891, 1971.

Hoffman, R. A., Auroral electron drift and precipitation: cause of the mantle aurora; J. Geophys. Res. (submitted for publication), 1971a.

Hoffman, R. A., Properties of low energy particle impacts in the polar domain in the dawn and dayside hours; presented at the Advanced Study Institute on Magnetosphere-Ionosphere Interactions, Dalseter, Norway April, 1971b.

Maynard, N. C., Electric fields in the ionosphere and magnetosphere; presented at the Advanced Study Institute on Magnetosphere-Ionosphere Interactions, Dalseter, Norway, April, 1971.

Sharp, R. D. and R. G. Johnson, Satellite measurements of auroral particle precipitation; Earth's Particles and Fields, ed. by B. M. McCormac, pp 113-125, Reinhold, New York, 1968.

Sugiura, M. and D. J. Poros, Hourly values of equatorial D_{ST} for the years 1957 to 1970; Goddard Space Flight Center Res. Rep. X-645-71-278, 1971.

Figure Captions

Plate 1a. Typical E-t spectrograms of electron intensities precipitated into the earth's atmosphere during periods of relative magnetic quiescence. These eight spectrograms have been ordered with respect to the local time of the observation with the noon and midnight sectors in the center top and bottom panels, respectively. The corresponding trajectories and Feldstein's auroral oval in Λ-MLT coordinates are displayed in the center panel.

Plate 1b. Continuation of Plate 1b for simultaneous observations of low-energy proton intensities precipitated into the upper atmosphere.

Note: Plates 1a and 1b to be published in color.

Figure 1. Directional intensities of trapped electrons ($E > 45$ keV) as functions of invariant latitude Λ for each of the eight spectrograms of Plates 1a and 1b. These measurements were used to delineate the trapping boundary as denoted by heavy arrows in the two color plates.

Figure 2. Interpretive diagram for the auroral zones and polar cap, including the low-altitude signatures

of plasma in the distant magnetosphere, the major convection zones and the field topology. (See text.)

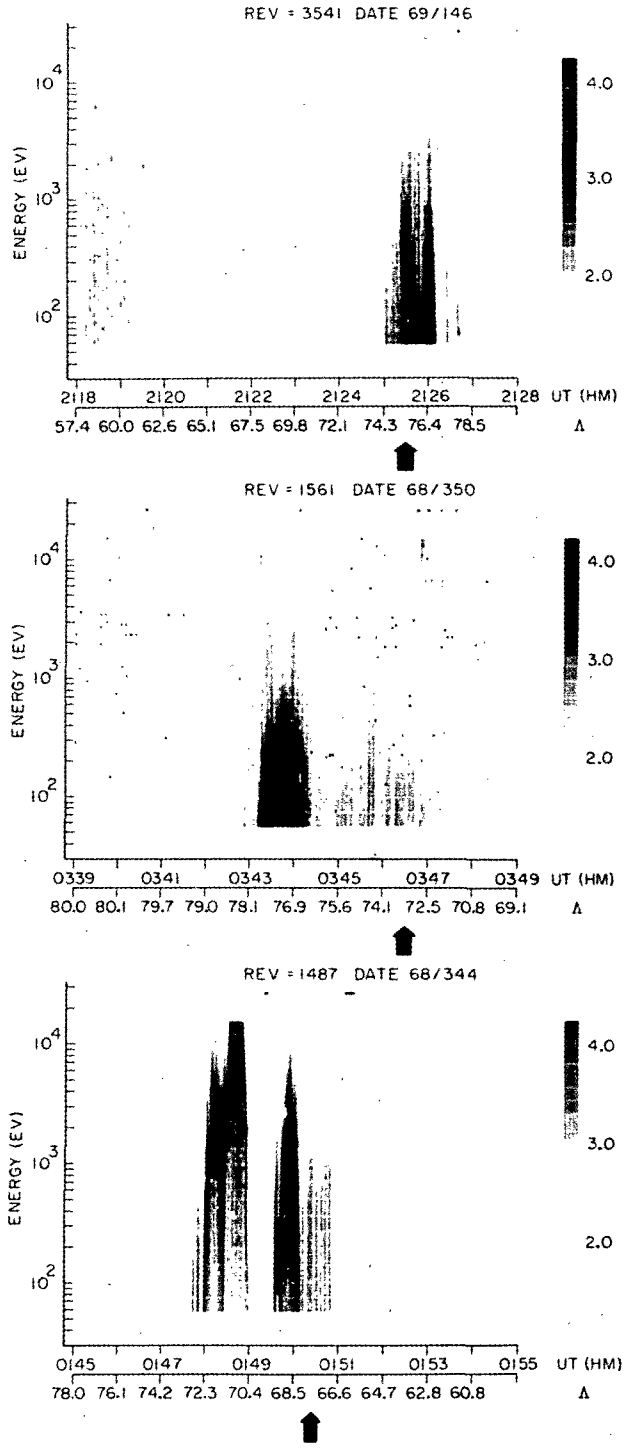
REV = 3541 DATE 69/146
ENERGY (EV)
10^4
10^3
10^2
4.0
3.0
2.0
2118 2120 2122 2124 2126 2128 UT (HM)
57.4 60.0 62.6 65.1 67.5 69.8 72.1 74.3 76.4 78.5 Λ
REV = 1561 DATE 68/350
0339 0341 0343 0345 0347 0349 UT (HM)
80.0 80.1 79.7 79.0 78.1 76.9 75.6 74.1 72.5 70.8 69.1 Λ
REV = 1487 DATE 68/344
0145 0147 0149 0151 0153 0155 UT (HM)
78.0 76.1 74.2 72.3 70.4 68.5 66.6 64.7 62.8 60.8 Λ

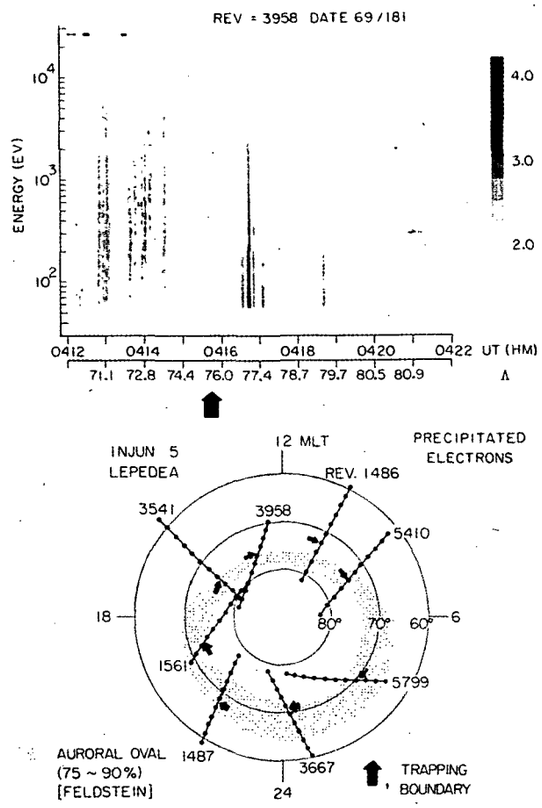
REV = 3958 DATE 69/181
ENERGY (EV)
10^4
10^3
10^2
4.0
3.0
2.0
0412 0414 0416 0418 0420 0422 UT (HM)
71.1 72.8 74.4 76.0 77.4 78.7 79.7 80.5 80.9 Λ
INJUN 5
LEPEDEA
12 MLT
PRECIPITATED
ELECTRONS
REV. 1486
3541
3958
5410
18
6
80°
70°
60°
1561
5799
AURORAL OVAL
(75 ~ 90%)
[FELDSTEIN]
1487
3667
24
TRAPPING
BOUNDARY
REV = 3667 DATE 69/157
ENERGY (EV)
10^4
10^3
10^2
4.0
3.0
2.0
0620 0622 0624 0626 0628 0630 UT (HM)
78.2 76.6 74.9 73.1 71.3 69.5 67.7 65.8 63.9 62.0 Λ

Plate 1a

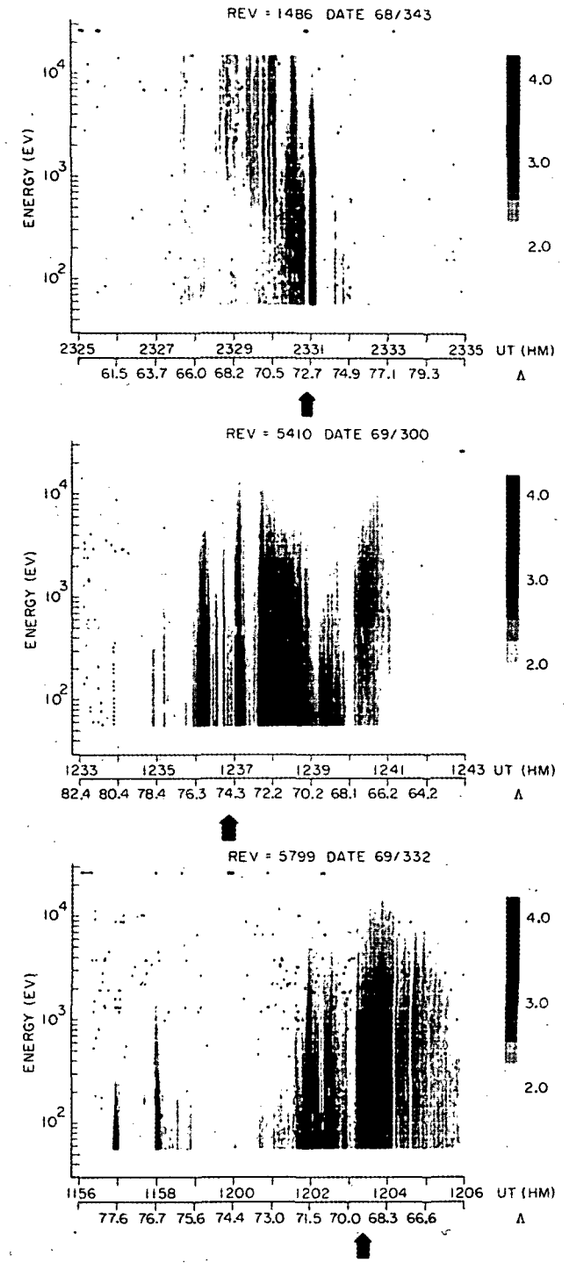
REV = 1486 DATE 68/343
ENERGY (EV)
10^4
10^3
10^2
4.0
3.0
2.0
2325 2327 2329 2331 2333 2335 UT (HM)
61.5 63.7 66.0 68.2 70.5 72.7 74.9 77.1 79.3 Λ
REV = 5410 DATE 69/300
ENERGY (EV)
10^4
10^3
10^2
4.0
3.0
2.0
1233 1235 1237 1239 1241 1243 UT (HM)
82.4 80.4 78.4 76.3 74.3 72.2 70.2 68.1 66.2 64.2 Λ
REV = 5799 DATE 69/332
ENERGY (EV)
10^4
10^3
10^2
4.0
3.0
2.0
1156 1158 1200 1202 1204 1206 UT (HM)
77.6 76.7 75.6 74.4 73.0 71.5 70.0 68.3 66.6 Λ

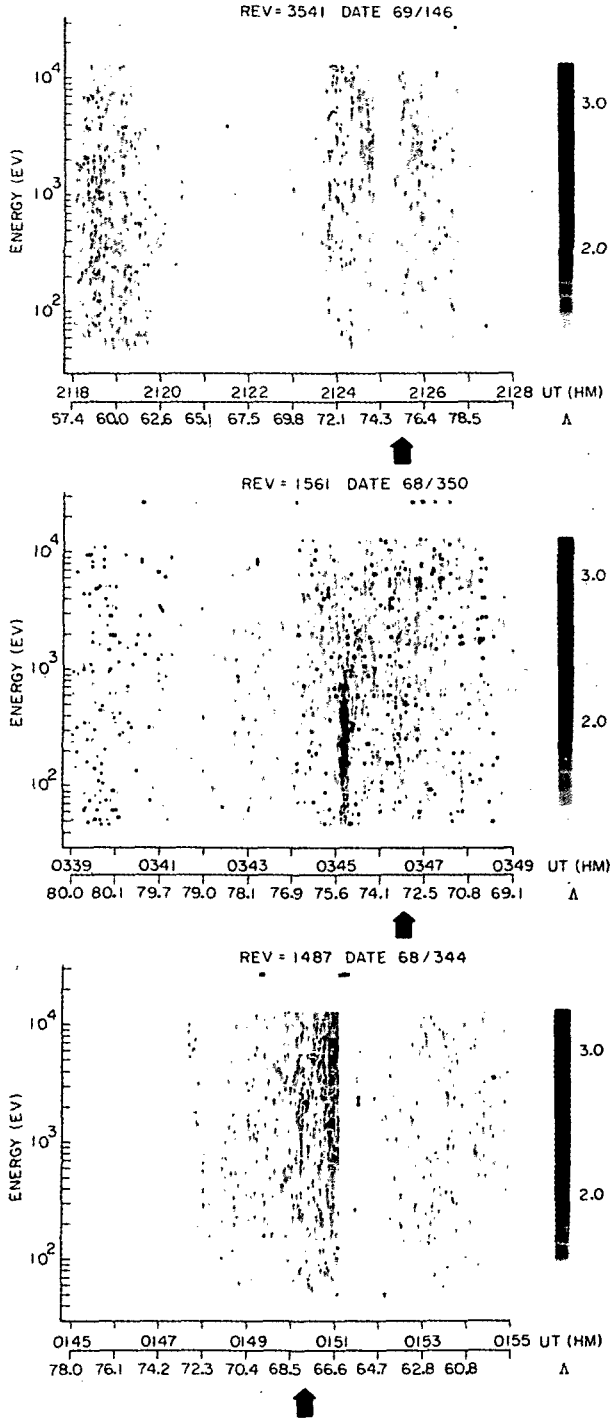
REV= 3541 DATE 69/146
ENERGY (EV)
10^4
10^3
10^2
3.0
2.0
2118 2120 2122 2124 2126 2128 UT (HM)
57.4 60.0 62.6 65.1 67.5 69.8 72.1 74.3 76.4 78.5 Λ
REV = 1561 DATE 68/350
0339 0341 0343 0345 0347 0349 UT (HM)
80.0 80.1 79.7 79.0 78.1 76.9 75.6 74.1 72.5 70.8 69.1 Λ
REV = 1487 DATE 68/344
0145 0147 0149 0151 0153 0155 UT (HM)
78.0 76.1 74.2 72.3 70.4 68.5 66.6 64.7 62.8 60.8 Λ

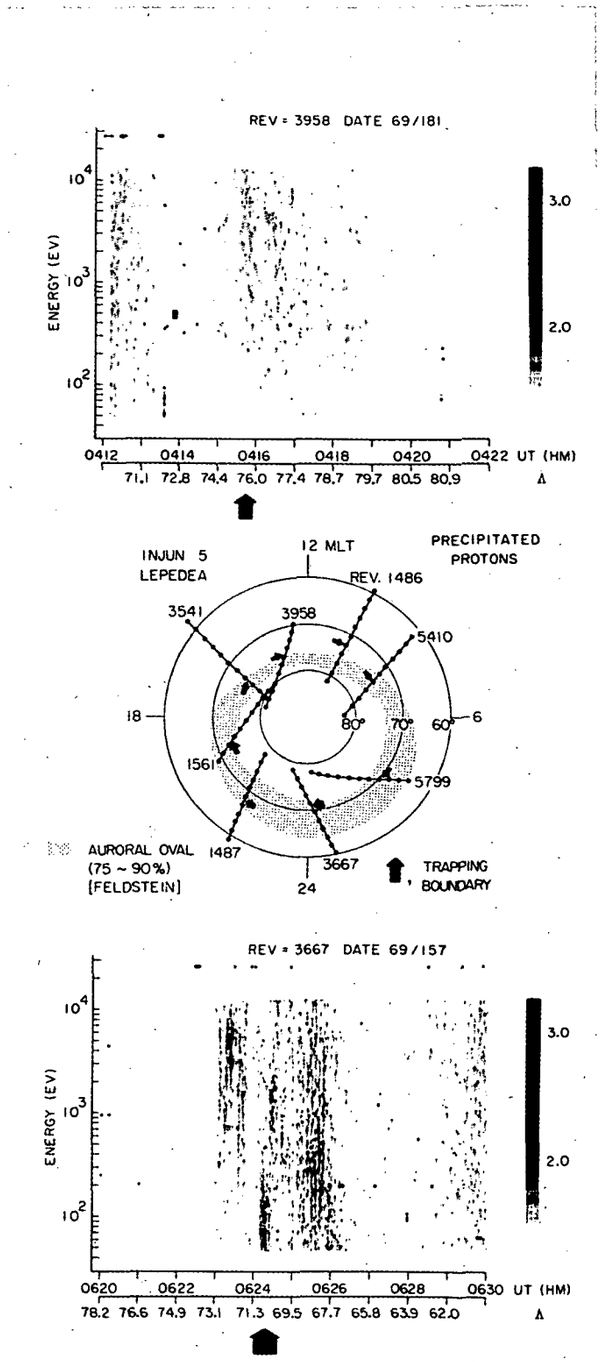
REV = 3958 DATE 69/181
ENERGY (EV)
10^4
10^3
10^2
3.0
2.0
0412 0414 0416 0418 0420 0422 UT (HM)
71.1 72.8 74.4 76.0 77.4 78.7 79.7 80.5 80.9 Λ
INJUN 5
LEPEDEA
12 MLT
PRECIPITATED
PROTONS
REV. 1486
3541
3958
5410
18
6
80°
70°
60°
1561
5799
1487
3667
24
AURORAL OVAL
(75 ~ 90%)
[FELDSTEIN]
TRAPPING
BOUNDARY
REV = 3667 DATE 69/157
ENERGY (EV)
3.0
2.0
0620 0622 0624 0626 0628 0630 UT (HM)
78.2 76.6 74.9 73.1 71.3 69.5 67.7 65.8 63.9 62.0 Λ

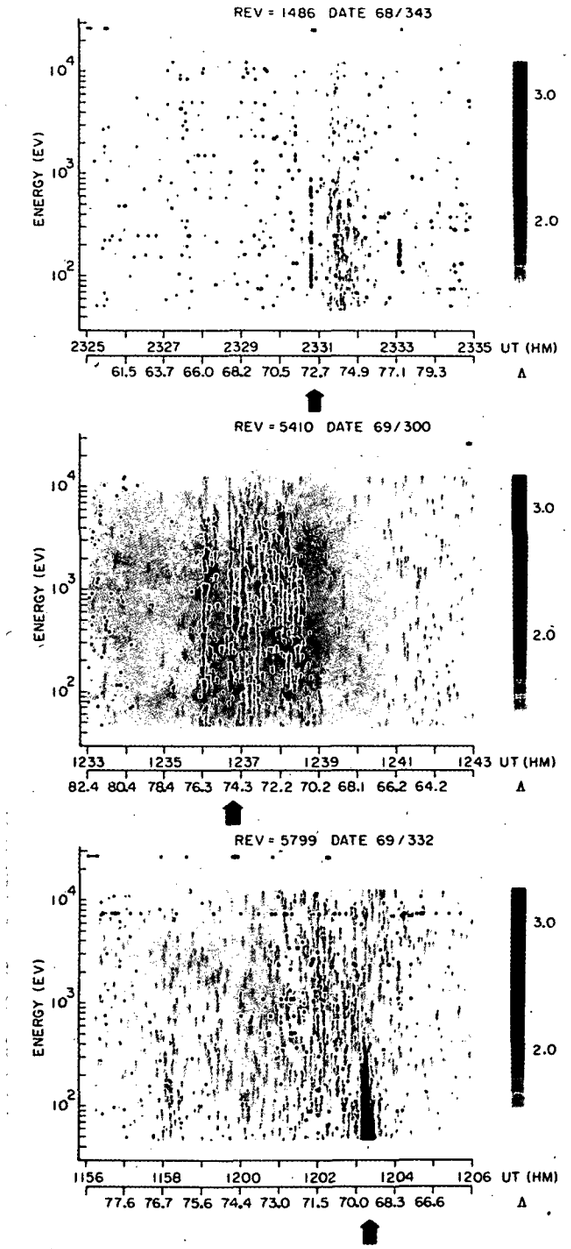
REV = 1486 DATE 68/343
ENERGY (EV)
10^4
10^3
10^2
3.0
2.0
2325 2327 2329 2331 2333 2335 UT (HM)
61.5 63.7 66.0 68.2 70.5 72.7 74.9 77.1 79.3 Λ
REV = 5410 DATE 69/300
1233 1235 1237 1239 1241 1243 UT (HM)
82.4 80.4 78.4 76.3 74.3 72.2 70.2 68.1 66.2 64.2 Λ
REV = 5799 DATE 69/332
1156 1158 1200 1202 1204 1206 UT (HM)
77.6 76.7 75.6 74.4 73.0 71.5 70.0 68.3 66.6 Λ

Plate 1b

C-G71-487

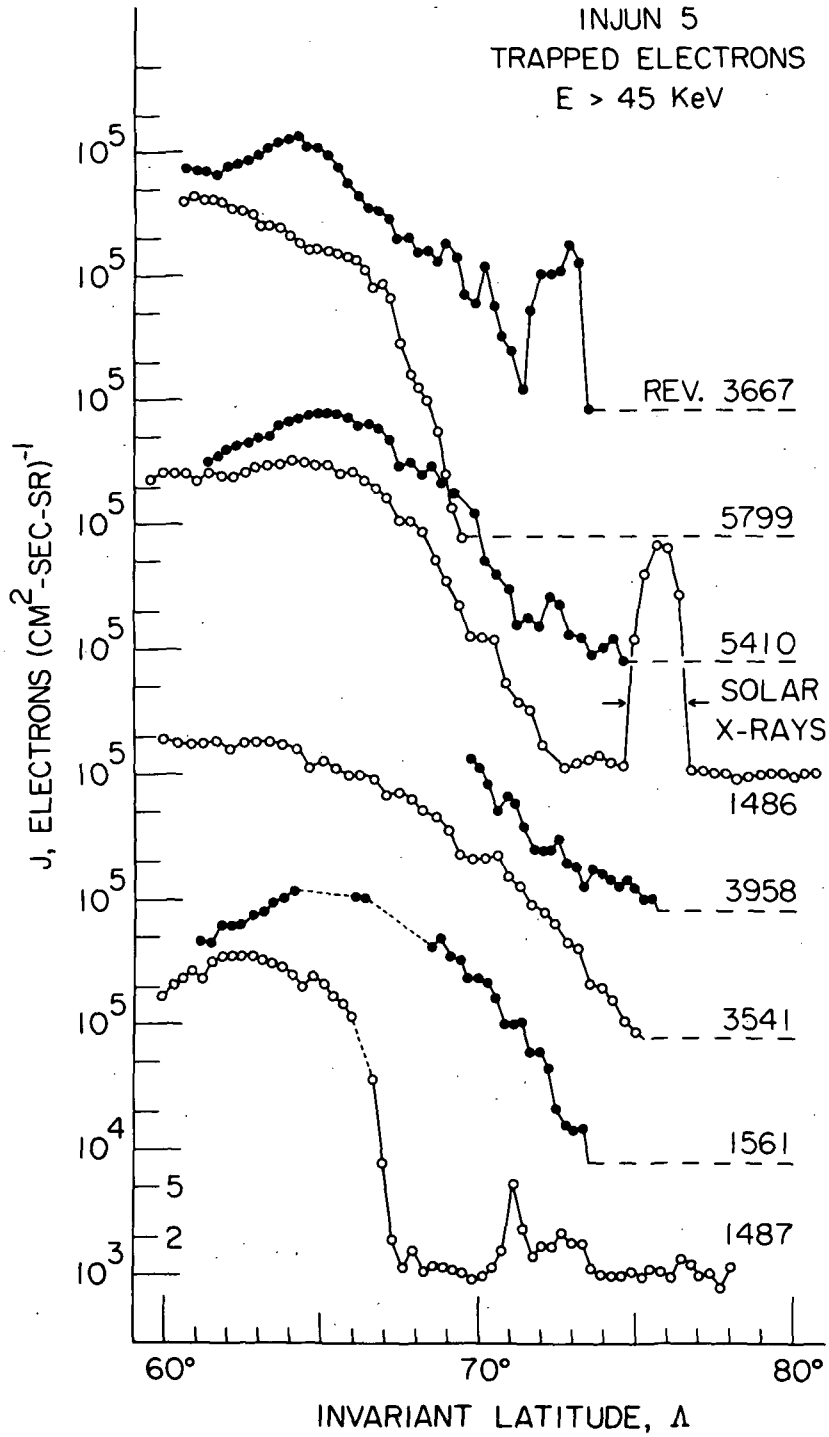

Figure 1

D-G71-165-1

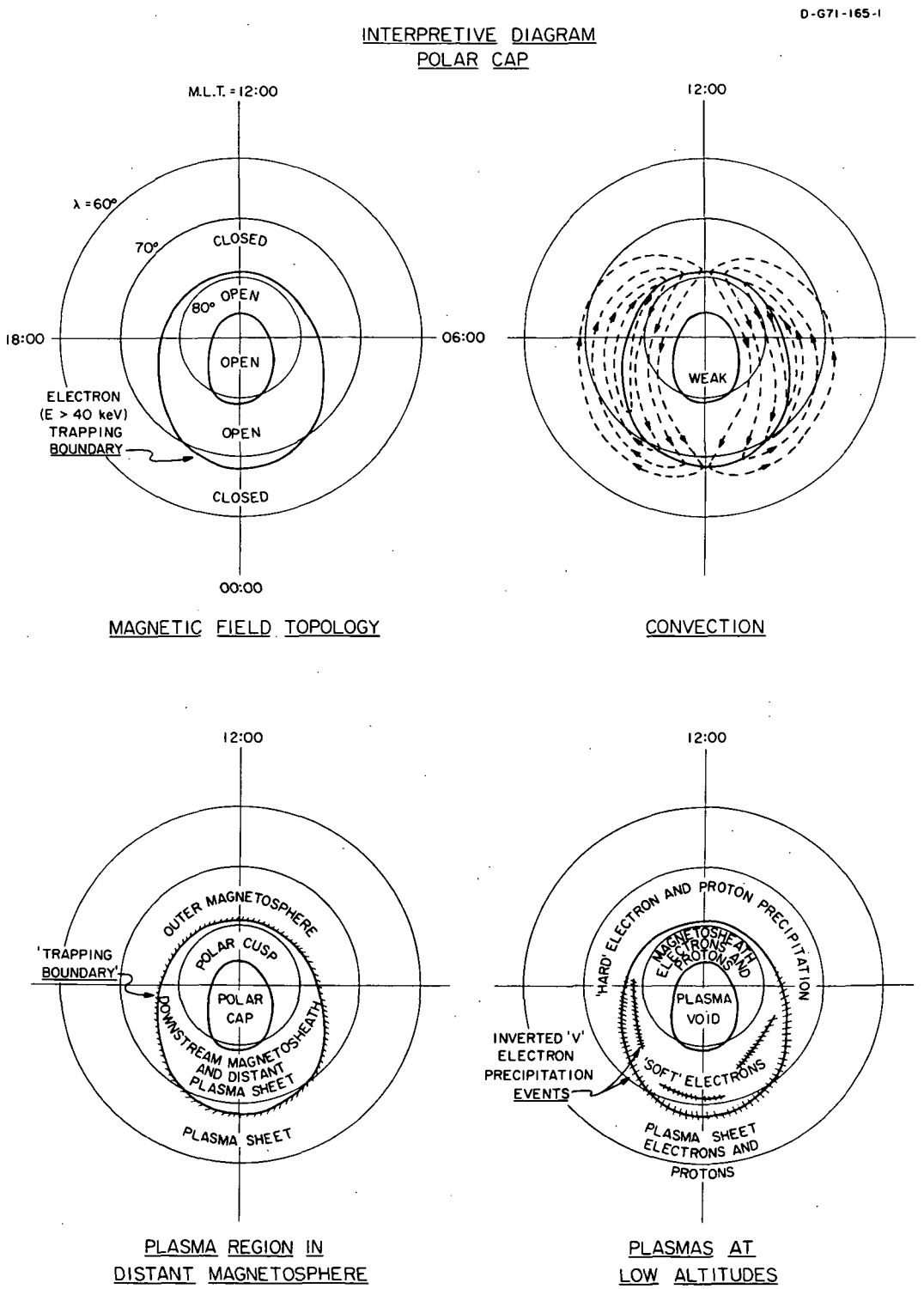

Figure 2